DISTINCTIVE CHARACTERISTICS OF GLACIAL ICE IN THE PR-GR SCATTER PLOTS OF AMSR-E NASA TEAM2 SEA ICE ALGORITHM

Hyangsun Han and Hoonyol Lee

Department of Geophysics, Kangwon National University, Republic of Korea

ABSTRACT

Sea ice concentration (SIC) calculated from the AMSR-E by using NASA Team2 (NT2) algorithm has proven to be very accurate over sea ice in Antarctic Ocean. When glacial ice such as icebergs and ice shelves are dominant in an AMSR-E footprint, the accuracy of NT2 algorithm is not well maintained. We extracted the concentrations of sea ice and glacial ice from two ENVISAT ASAR images of southern Antarctica, and compared them with NT2 SIC. The result showed that the NT2 algorithm underestimates the concentration of glacial ice. We also found that glacial ice occupies a unique region in the PR (polarization ratio), GR (spectral gradient ratio), PR_R (rotated PR), and ΔGR domain different from other types of ice such as ice type A, B, and C, and open water. This implies that glacial ice concentration can be added as a new category of ice to the NT2 algorithm.

Index Terms— AMSR-E, sea ice concentration, NASA Team2 algorithm, glacial ice, glacial ice concentration

1. INTRODUCTION

The glacial ice, which is originated from fresh water, is formed to appear as ice sheets, ice shelves, glaciers, and icebergs when the snow is precipitated, accumulated, and compressed on land for a long time. Based on the source of the ice formation, the glacial ice is has different microwave radiation properties from the sea ice frozen from salty water [1]. Glacial ice is closely related to the global warming. In the Antarctic, rapid decrease in glaciers and ice shelves is distinctly observed. The glacial ice is flowed into ocean that changes coastal landform and the environment of sea ice formation. It is very important to detect discharge rate of glacial ice by observing icebergs floating at sea effectively for the study of mass-balance of polar ice, not to mention the navigational safety issue.

Passive microwave sensors onboard satellites are very useful to observe polar ice because they can provide daily sea ice concentration over ocean around of the Arctic and Antarctic. AMSR-E, is a typical passive microwave sensor, provides daily sea ice concentration by using NASA Team2 (NT2) algorithm with 12.5 km spatial resolution from 2002 to present [2]. Although NT2 algorithm has better spatial resolution and accuracy of ice concentration than NASA Team sea ice algorithm used in SSM/I, it may have low accuracy over the glacial ice region because glacial ice has the different radiation characteristics from sea ice and open water [3] and the sea ice algorithm did not accounted for the effect of glacial ice so far.

In this paper we studied microwave radiation properties of glacial ice based on scatter plots of PR (polarization ratio), GR (spectral gradient ratio), PR_R (rotated PR), and ΔGR which are used to classify ice types and calculate ice concentration in NASA Team2 algorithm. We compared ENVISAT ASAR images with AMSR-E NT2 sea ice concentration. We then analyzed the microwave radiation properties of glacial ice.

2. DATA AND METHOD

We used two ENVISAT ASAR wide swath images obtained over the George V Coast in the southern Antarctica adjacent to the Pacific Ocean on 20 and 26 April, 2006. All ASAR images are obtained as HH polarization and by descending orbit. In the ASAR images, most sea surface was covered with sea ice and there are several icebergs and an ice shelf (Fig. 1a). The distinction between sea ice and ice shelf was difficult by ASAR images alone, but we could confirm the ice shelf region through time-series MODIS images.

We masked inland in the ASAR images using the land mask product of the NT2 algorithm and classified ice type into sea ice, icebergs, and ice shelf by supervised classification and digitizing. We calculated the concentration of sea ice, icebergs, and ice shelf from two ASAR images. The overall accuracy of the classification in each ASAR image is 97.4% and 94.4%, respectively (Table 1).

AMSR-E onboard on Aqua is a passive microwave sensor which is composed of 6.9, 10.7, 18.7, 23.8, 36.5, and 89.0 GHz dual polarized channels. AMSR-E measures microwave radiation intensity of the polar ice. AMSR-E provides sea ice concentration with 12.5 km resolution by using NT2 algorithm. National Snow and Ice Data Center (NSIDC) provides AMSR-E Brightness Temperature (T_B) and NT2 sea ice concentration of daily-averaged, day-time

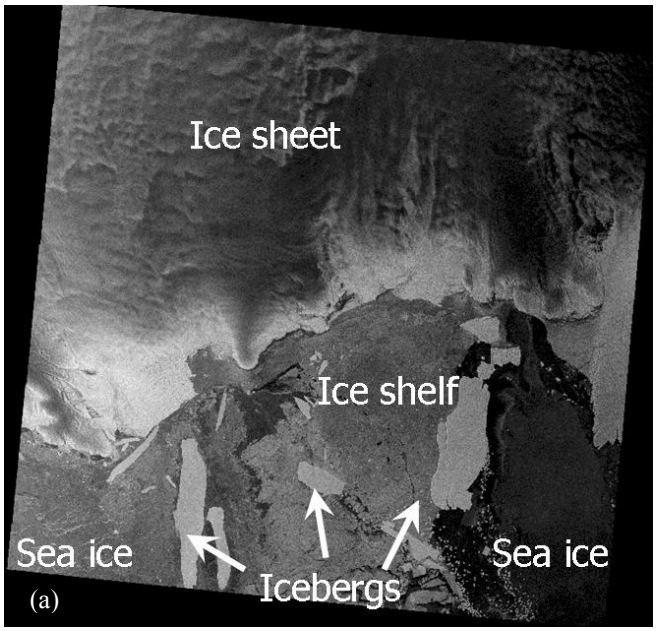

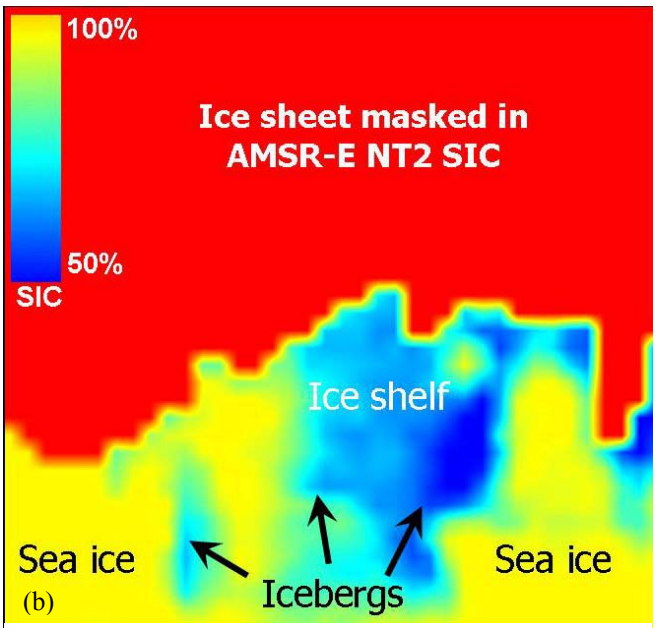

Fig. 1 (a) ENVISAT ASAR images of study area obtained on 26 April, 2006. (b) AMSR-E NASA Team2 sea ice concentration image obtained on 26 April, 2006. The sea ice concentration is nearly 100% but the glacial ice concentration is underestimated in NT2 sea ice concentration image.

(ascending orbit), and night-time (descending orbit) products. We obtained the AMSR-E NT2 sea ice concentration and the T_B data products of the same dates as the ASAR images (Fig. 1b).

NT2 algorithm identifies ice type A, B, and C, and open water by plotting data in PR, GR, PR_R, and ΔGR domain. The PR and GR is calculated as [2]

$$PR(\nu) = \frac{\left(T_B(\nu,V) - T_B(\nu,H)\right)}{\left(T_B(\nu,V) + T_B(\nu,H)\right)} \tag{1}$$

$$GR(\nu_1 p\ \ \nu_2 p) = \frac{\left(T_B(\nu_1,p) - T_B(\nu_2,p)\right)}{\left(T_B(\nu_1,p) + T_B(\nu_2,p)\right)}$$

where ν is the channel and p is the polarization. In NT2 sea ice algorithm, PR(18) and GR(37V18V) domain is used to identify sea ice types and open water. Sea ice has smaller value of both PR(18) and GR(37V18V) when compared with open water that has high PR and GR. The PR and GR of snow layer on ice surface are similar to open water [4].

In order to classify the ice type that has large surface effect by snow layer (i.e., ice type C), NT2 algorithm uses PR_R and ΔGR. The $PR_R(18)$ and ΔGR is calculated as [2]

$$PR_R(18) = PR(18)\cos\phi - GR(37V18V)\sin\phi \tag{2}$$

$$\Delta GR = GR(89H18H) - GR(89V18V)$$

where ϕ is the angle between GR-axis and 100% of ice type A-B line (Fig. 2a). In the Antarctic, the ϕ is -0.59 radians. ΔGR is the difference between GR(89H18H) and GR(89V18V). The value of PR (18) of ice type C is close to the value of open water. The $PR_R(18)$, however, maintains small value close to 0 in ice type C. Generally, the value of ΔGR of sea ice is close to 0 because the GR(89H18H) of sea ice is similar to the GR(89V18V).

As the variation of daily temperature can change the radiation property, we` excluded pixels of AMSR-E data that have large change in sea ice concentration and T_B products. However, sea ice on Antarctic Ocean in this winter season was spatially and temporally stable [1]. When observed by the ASAR images, the ocean surface was mostly covered with sea ice with a little open water by narrow cracks.

In the sea ice region, the difference between ASAR ice concentration and AMSR-E NT2 sea ice concentration was very small by 1.4% of RMSE. The NT2 algorithm, however, underestimates ice concentration on glacial ice by 26.4% of RMSE. To interpret the large deviation of estimation over

Table 1. The classification accuracy of the ASAR images.

	User accuracy		Producer accuracy		Overall accuracy
	Ice	Open water	Ice	Open water	
2006/04/20	98.5%	84.1%	98.7%	82.7%	97.4%
2006/04/26	96.4%	86.7%	96.6%	85.7%	94.4%

glacial ice, we analyzed the characteristics of microwave radiation of the glacial ice in PR, GR, PR_R, and ΔGR domain.

3. RESULT AND DISCUSSION

Fig. 2 (a) shows the scattergram between PR(18) and GR(37V18V) of sea ice (black dots) and glacial ice (blue dots). The vertices of a triangle represent ice type A, B, and open water, respectively. Ice type A in the Antarctic Ocean is similar to first-year ice in the Arctic Ocean. Ice type B, which is similar to multi-year ice in the central Arctic Ocean, has thick snow cover and is mostly found at Weddell Sea. Most sea ice around the Antarctica is ice type A because the sea ice thaws completely during summertime.

High PR(18) is a typical signature of new ice or snow layer on sea ice that reduces sea ice concentration [4]. New ice has similar characteristics with open water because of its thin ice thickness. When sea ice is covered with a snow layer (ice type C), the radiance of 18.7 GHz horizontal polarization reduces so that higher PR(18) is calculated than a sea ice without snow cover. GR(37V18V) of ice type C has negative value between ice type A and B. The equi-concentration lines of sea ice are parallel to the side of the triangle connecting points of ice type A and B.

The average of PR(18) from glacial ice was calculated as 0.072 (Table 2), which is larger than the average value of sea ice (0.048). GR(37V18V) from glacial ice was also higher than sea ice. In general, glacial ice forms a unique cluster in the GR(37V18V)-PR(18) domain against any other types of ice and open water used in the NT2 algorithm.

Fig. 2 (b) shows the scattergram between GR(89H18H) and GR(89V18V) of sea ice (black dots) and glacial ice (blue dots). The black line is 100% of sea ice concentration while the black-circled area corresponds to open water. Glacial ice form a unique cluster in the GR(89H18H) and GR(89V18V) domain.

GR(89H18H) and GR(89V18V) of glacial ice are generally higher than those of sea ice due to the difference of radiation property of glacial ice and sea ice at 89.0 GHz and 18.7 GHz. The T_B of 89.0 GHz channel from glacial ice is warmer than sea ice [5]. Moreover, the T_B of 18.7 GHz channel from glacier ice is smaller than that from sea ice [6]. This is because 89.0 GHz observes the T_B radiating from air/ice interface or the upper layer of ice while 18.7 GHz can detects radiation from lower ice layer as well. The radiation of 18.7 GHz from the lower glacial ice layer is diffused in the upper ice layers. Therefore the observed T_B of 18.7 GHz from thick glacial ice is generally smaller than that from the relatively thinner sea ice.

Fig. 2 (c) shows the scatter plot of $PR_R(18)$ and ΔGR of sea ice (black dots) and glacial ice (blue dots). The values of ΔGR of glacial ice are generally higher than those of sea ice. The value of $PR_R(18)$ of the sea ice is closer to 0 than the glacial ice. The $PR_R(18)$ is used to improve the accuracy of

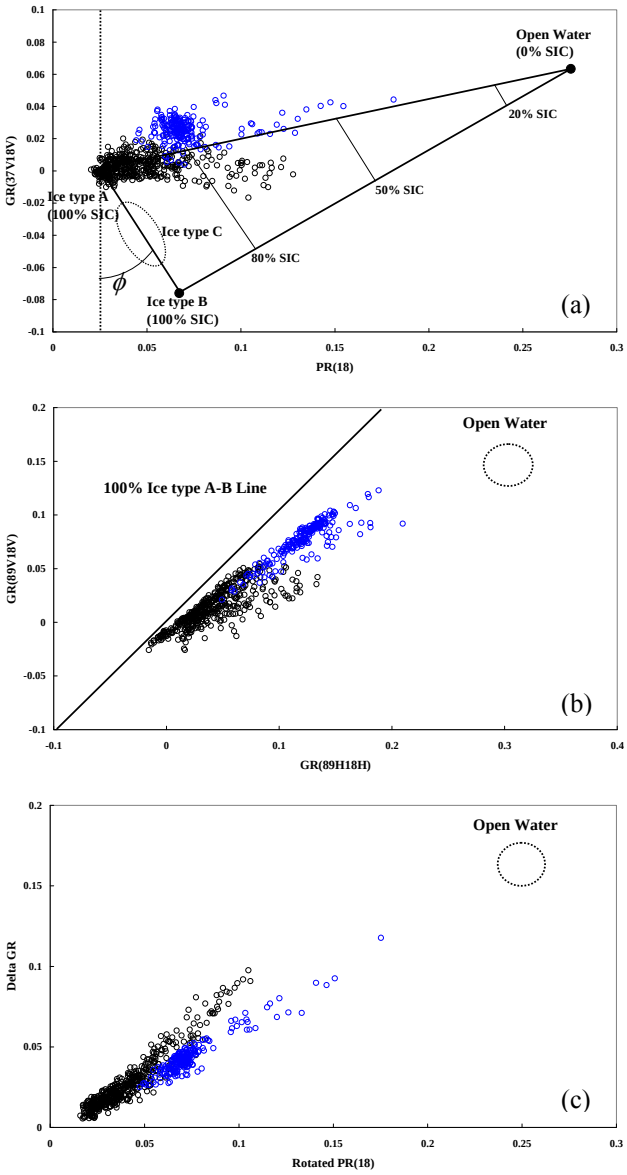

Fig. 2 (a) Scatter plot of PR(18) and GR(37V18V) of sea ice (black dots) and glacial ice (blue dots). (b) Scatter plot of GR(89H18H) and GR(89V18V) of sea ice (black dots) and glacial ice (blue dots). (c) Scatter plot of $PR_R(18)$ and ΔGR of sea ice (black dots) and glacial ice (blue dots). The glacial ice forms a unique cluster in the PR-GR and PR_R-ΔGR domain.

Table 2. Statistics of the AMSR-E PR, GR, PR_R, and ΔGR.

		Sea ice	Glacial ice
PR(18)	Avg.	0.048	0.072
	Std.	0.019	0.020
	Max.	0.128	0.181
	Min.	0.021	0.044
	Mdn.	0.042	0.068
GR(37V18V)	Avg.	0.004	0.025
	Std.	0.007	0.008
	Max.	0.028	0.048
	Min.	-0.017	0.004
	Mdn.	0.004	0.025
GR(89V18V)	Avg.	0.016	0.074
	Std.	0.020	0.021
	Max.	0.071	0.123
	Min.	-0.026	0.016
	Mdn.	0.013	0.076
GR(89H18H)	Avg.	0.044	0.118
	Std.	0.030	0.030
	Max.	0.134	0.211
	Min.	-0.016	0.046
	Mdn.	0.040	0.120
$PR_R(18)$	Avg.	0.042	0.074
	Std.	0.017	0.019
	Max.	0.106	0.175
	Min.	0.016	0.045
	Mdn.	0.038	0.070
ΔGR	Avg.	0.028	0.044
	Std.	0.016	0.014
	Max.	0.098	0.118
	Min.	0.006	0.021
	Mdn.	0.024	0.042

concentration of the ice type C. $PR_R(18)$ of the ice type A and B, as well as ice type C, is close to 0. The glacial ice forms a unique cluster which has generally higher values of $PR_R(18)$ than sea ice. This implies that the glacial ice has different microwave radiation properties from the sea ice and it can be classified into a new ice type in PR_R-ΔGR domain.

Through this study, we found that glacial ice can be uniquely identified in PR-GR and PR_R-ΔGR domain apart from other sea ice types and open water used in the NT2 sea ice algorithm.

4. CONCLUSION

We evaluated the AMSR-E NASA Team2 (NT2) sea ice concentration in a region of southern Antarctic. We found that AMSR-E NT2 algorithm underestimates the ice concentration over the regions of glacial ice such as ice shelf and icebergs. Glacial ice showed higher PR(18), GR(37V18V), GR(89V18V), GR(89HV18H), $PR_R(18)$, and ΔGR values than those of sea ice. Through analysis of the PR-GR and PR_R-ΔGR scatter plot, we found that the glacial ice forms a unique cluster against sea ice and open water.

We are planning to analyze microwave radiation properties of glacial ice in various seasons and regions, and to improve the accuracy of AMSR-E NT2 algorithm by adding Glacial Ice Concentration (GIC). GIC can also be used for the study of improvement in land-masking of AMSR-E products, iceberg tracking, and monitoring of coastal landform by the movement of glacial ice.

ACKNOWLEDGMENTS

This research was supported by Basic Science Research Program through the National Research Foundation of Korea (NRF) funded by the Ministry of Education, Science and Technology (No. 2010-0009465).

REFERENCES

[1] H. Lee, and H. Han, "Evaluation of SSM/I and AMSR-E sea ice concentrations in the Antarctic spring using KOMPSAT-1 EOC imagery," *IEEE Transactions on Geoscience and Remote Sensing*, vol. 46, no. 7, pp. 1905-1912, 2008.

[2] T. Markus, and D. J. Cavalieri, "An enhancement of the NASA Team sea ice algorithm," *IEEE Transactions on Geoscience and Remote Sensing*, vol. 38, no. 3, pp. 1387-1898, 2000.

[3] S. Andersen, L. Kaleschke, G. Heygster, and L. T. Pedersen, "Intercomparison of passive microwave sea ice concentration retrievals over the high-concentration Arctic sea ice," *Journal of Geophysical Research*, doi:10.1029/2006JC003543, 2007.

[4] T. Markus, D. J. Cavalieri, A. J. Gasiewski, M. Klein, J. A. Maslanik, D. C. Powell, B. B. Stankov, J. C. Stroeve, and M. Sturm, "Microwave signatures of snow on sea ice: Observations", *IEEE Transactions on Geoscience and Remote Sensing*, vol. 44, no. 11, pp. 3081-3090, 2006.

[5] S. Martin, R. S. Drucker, and R. Kwok, "The areas and ice production of the western and central Ross Sea polynyas, 1992-2002, and their relation to the B-15 and C-19 iceberg events of 2000 and 2002," *Journal of Marine Systems*, vol. 68, no. 1-2, pp. 201-214, 2007.

[6] L, Jiang, J. Shi, S. Tjuatja, J. Dozier, K. Chen, and L. Zhang, "A parameterized multiple-scattering model for microwave emission from dry snow," *Remote Sensing of Environment*, vol. 111, no. 2-3, pp. 357-366, 2007.